Journal of Thermal Analysis and Calorimetry, Vol. 64 (2001) 1001–1010

PHASE FORMATION STUDY OF THE SUBSTITUTED LANTHANUM MANGANITES SOLID SOLUTIONS

A. Ianculescu[1], *A. Braileanu*[1], *M. Zaharescu*[1], *I. Pasuk*[2], *E. Chirtop*[3], *C. Popescu*[4] *and E. Segal*[5]

[1]Institute of Physical Chemistry, 202 Spl. Independentei, 77208 Bucharest, Romania
[2]SC ICPE SA., 313 Spl. Unirii, 74204 Bucharest, Romania
[3]SC MATPUR SA., 41-45 Drumul intre tarlale, 73611 Bucharst, Romania
[4]LACECA Research Centre, 95 Siret, 78308 Bucharest, Romania
[5]University of Bucharest, Faculty of Chemistry, Department of Physical Chemistry, 13 Blv. Republicii, Bucharest, Romania

Abstract

It is well known that the manganites-based solid solutions are interesting for their electric and magnetic properties. $LaMnO_3$ exhibits a distorted perovskite structure due to Mn^{3+} ion, which determines the presence of the Jahn–Teller effect. Replacing La^{3+} host ions by cations of lower valence leads to the disappearance of this effect and changes the characteristics of these materials.

Although the formation of manganites-based solid solutions has been intensively studied, there are some unelucidated aspects concerning their formation mechanism, depending both on the precursors used and on the thermal treatment applied in order to obtain suitable properties.

In this work the formation mechanism of $La_{0.7}M_{0.3}MnO_3$ (M=Ca, Sr, Ca+Sr in equimolecular mixture) solid solutions, in isothermal and non-isothermal conditions, was studied. For this purpose XRD, DTA/TG and spectral techniques were used. The solid solutions formation was found to be more dependent on the Mn-precursors type than the thermal treatment conditions.

Keywords: manganite, perovskite, solid solution, thermal analysis, XRD

Introduction

Solid solutions in the La_2O_3–Mn_2O_3–MO system have been intensively investigated [1–4] due to their interesting applications. The most important compound of the system is $LaMnO_3$ with distorted perovskite structure (ABO_3 with A=La and B=Mn) due to Jahn–Teller effect and with a high value of the *p*-type electric conductivity due to its non-stoichiometry with high concentration of cation vacancies [5]. $LaMnO_3$ doped with alkaline-earth ions is successfully used as semiconducting material for the cathode of fuel cells with solid electrolyte (SOFC) while the solid solutions obtained by substitution of manganese by chromium are used as interconnecting materials [1].

1418–2874/2001/ $ 5.00
© 2001 Akadémiai Kiadó, Budapest

Akadémiai Kiadó, Budapest
Kluwer Academic Publishers, Dordrecht

Experimental

Pure $LaMnO_3$, as reference, as well as the solid solutions $La_{1-x}M_xMnO_3$ (M=Ca, Sr, Ca+Sr; x=0.3) were prepared by classical solid state method from high purity (>99.9%) oxides, carbonates and acetates as: La_2O_3, MnO_2, $MnCO_3$, $Mn(CH_3COO)_2\cdot 4H_2O$, $CaCO_3$ (Merck) and $SrCO_3$ (Fluka).

The analyzed compositions are presented in Table 1.

Table 1 Composition of investigated $La_{1-x}M_xMnO_3$ solid solutions

Symbol	Formula	Manganese precursor
LM_1	$LaMnO_3$	MnO_2
LCM_1	$La_{0.7}Ca_{0.3}MnO_3$	
LSM_1	$La_{0.7}Sr_{0.3}MnO_3$	
$LCSM_1$	$La_{0.7}Ca_{0.15}Sr_{0.15}MnO_3$	
LM_2	$LaMnO_3$	$Mn(CH_3COO)_2\cdot 4H_2O$
LCM_2	$La_{0.7}Ca_{0.3}MnO_3$	
LSM_2	$La_{0.7}Sr_{0.3}MnO_3$	
$LCSM_2$	$La_{0.7}Ca_{0.15}Sr_{0.15}MnO_3$	
LM_3	$LaMnO_3$	$MnCO_3$
LCM_3	$La_{0.7}Ca_{0.3}MnO_3$	
LSM_3	$La_{0.7}Sr_{0.3}MnO_3$	
$LCSM_3$	$La_{0.7}Ca_{0.15}Sr_{0.15}MnO_3$	

The raw materials were proportioned, homogenized by wet procedure in a planetary ball mill using ethanol as dispersing medium and then dried.

In order to study the changes which occur during thermal treatment, thermal analysis of raw materials as well of the mentioned mixtures were performed. The powders were heated in static air atmosphere from ambient temperature until 1000°C with 5°C min^{-1}. In order to clarify the solid solution formation mechanism and to establish the composition of the intermediate compounds, the initial mixtures were submitted to some non-isothermal treatments until various temperatures (550, 650, 850°C). The quenched powders were analyzed by X-ray diffraction.

The mixtures were shaped by uniaxially pressing at 100 MPa into pellets of ϕ=20 mm and h=2–3 mm and thermally treated in air, in temperature range of 1000–1300°C with 3 h plateau. The phase composition as well as the phase formation were studied by X-ray diffraction using the CuK_α radiation. The same method was used for the structural characterization of manganites obtained from oxide precursor (MnO_2).

The evolution of manganites structure as function of dopant type and manganese precursor were investigated by infrared spectroscopy (IR), too.

Results and discussions

Differential thermal analysis

Table 2 shows the DTA data for the raw materials used.

Table 2 Thermal behavior of the raw materials used

Raw material	Thermal effect/°C		Assignment
	endo	exo	
La_2O_3	380		$La(OH)_3$ dehydration
	530		$La_2O_2 \cdot CO_3$ decomposition
	700		$La_2O_2 \cdot CO_3$ decomposition
MnO_2	595, 615		$MnO_2 \rightarrow Mn_2O_3$ reduction
	950		$Mn_2O_3 \rightarrow Mn_3O_4$ reduction
$Mn(CH_3COO)_24H_2O$	100, 130		$Mn(CH_3COO)_2 \cdot 4H_2O$ dehydration
		310, 365	$Mn(CH_3COO)_2$ decomposition +organic material combustion
	900		$Mn_2O_3 \rightarrow Mn_3O_4$ reduction
$MnCO_3$	382		$MnCO_3 \rightarrow MnO_2$ decomposition
	550, 582		$MnO_2 \rightarrow Mn_2O_3$ reduction
	950		$Mn_2O_3 \rightarrow Mn_3O_4$ reduction
$CaCO_3$	758		$CaCO_3$ decomposition
$SrCO_3$	878		rhombohedral→hexagonal $SrCO_3$ phase transition
	1052		$SrCO_3$ decomposition

MnO_2 precursor

For all these mixtures (LM_1, LCM_1, LSM_1, $LCSM_1$), DTA curves show the thermal effects characteristic of the raw materials listed in Table 2, with lower temperatures of alkaline earth carbonates decomposition. Differences appear in the temperature range 640–830°C, being significant for the mixtures LM_1 and LCM_1 (Fig. 1).

For the LM_1 mixture, a flattened endothermic effect with two minima (690 and 770°C) appears, assigned to the decomposition of $La_2O_2CO_3$ simultaneously with the $LaMnO_3$ perovskite skeleton formation, by solid phase reaction: $La_2O_2CO_3+Mn_2O_3 \rightarrow LaMnO_3+CO_2$.

For the mixture LCM_1 the same endothermic effect, but more marked due to its superposition with $CaCO_3$ decomposition was evidenced.

DTA curves of the mixtures with Sr dopant (LSM_1 and $LCSM_1$) show the characteristic decomposition effect of $SrCO_3$, which occurs at lower temperature (~940^{O}C) than the one specific to pure $SrCO_3$ (1052°C). This effect is difficult to be assigned because of its overlapping with the $Mn_2O_3 \rightarrow Mn_3O_4$ reduction effect detected at the same temperature.

In case of the $LCSM_1$ mixture, $CaCO_3$ and $SrCO_3$ decomposition effects are weaker because of the lower amount of calcium and strontium admixtures compared to the LCM_1

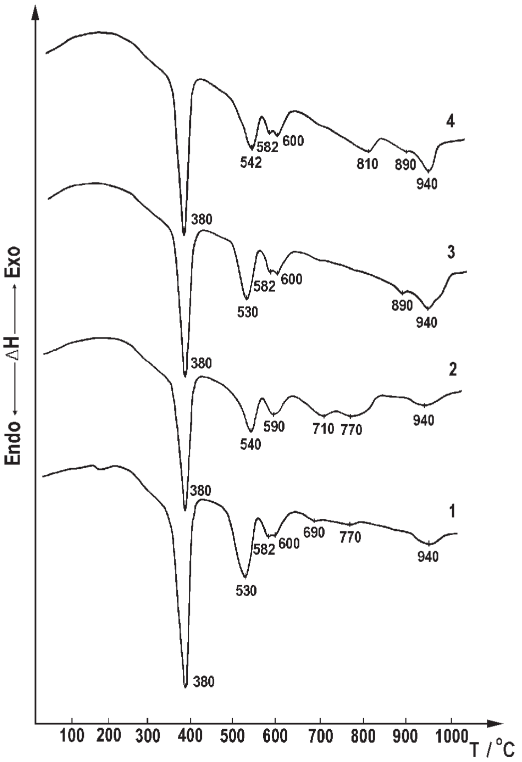

Fig. 1 DTA curves for the mixtures prepared with MnO_2 as precursor: 1 – LM_1; 2 – LCM_1; 3 – LSM_1; 4 – $LCSM_1$

and LSM_1, respectively. However, the presence of calcium is detectable by the more intense reaction of perovskite skeleton formation than that of the LSM_1 one.

$Mn(CH_3COO)_2$ precursor

The DTA curves of the mixtures LM_2, LCM_2, LSM_2 and $LCSM_2$ show that the dehydration of $La(OH)_3$ is not evidenced because of its superposition with the decomposition and combustion effects of manganese acetate. In this case the complex process of $La_2O_2CO_3$ decomposition simultaneously with the formation of perovskite skeleton is less pronounced, taking place in a large temperature range. The presence of the perovskite skeleton is mentioned in literature [6] and was emphasized by us using X-ray diffraction for the thermally treated powders until 650°C (Fig. 2).

$MnCO_3$ precursor

All the mixtures (LM_3, LCM_3, LSM_3, $LCSM_3$) exhibit on the DTA curves the endothermic effects at 380°C on the DTA curves, dehydration of $La(OH)_3$, ~810°C (effect which is going to be discussed) and 910°C (reduction of Mn_2O_3 to Mn_3O_4). The mixtures containing calcium and strontium exhibit their specific thermal effects, too. The temperature range of interest is 500–820°C (Fig. 3).

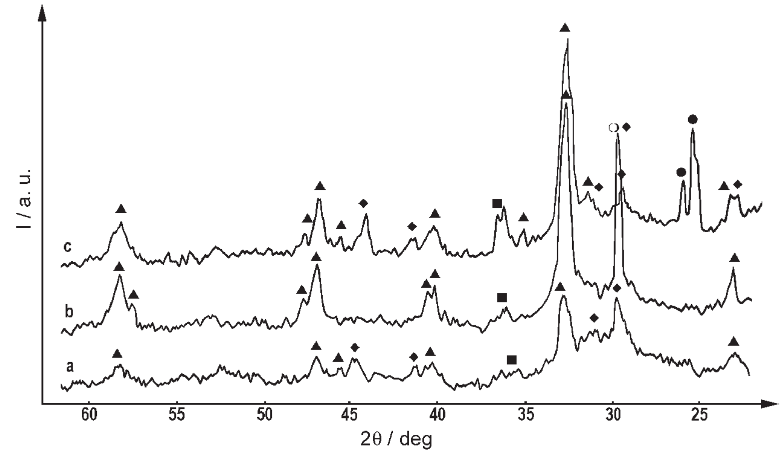

Fig. 2 X-ray diffraction patterns for mixtures thermally treated at 650°C using $Mn(CH_3COO)_2$ as precursor: a – LM_2; b – LCM_2; c – LSM_2 (▲ – $LaMnO_3$, ◆ – $La_2O_2CO_3$, ● – $SrCO_3$, o – $CaCO_3$, ■ – Mn_2O_3)

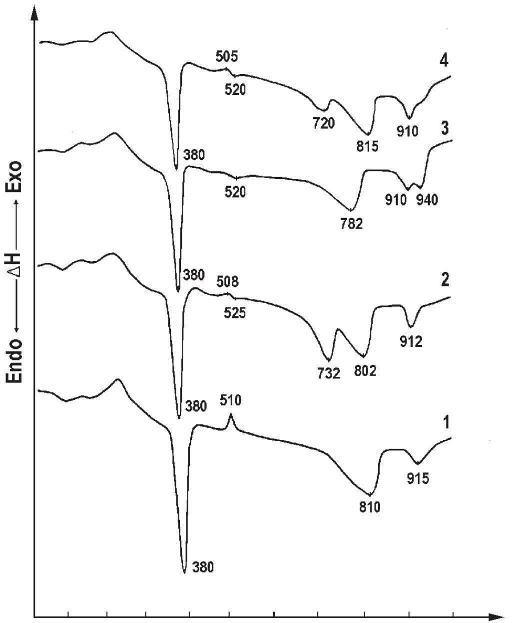

Fig. 3 DTA curves for the mixtures obtained with $MnCO_3$ as precursor: 1 – LM_3; 2 – LCM_3; 3 – LSM_3; 4 – $LCSM_3$

The DTA curve of the mixture LM_3 shows an exothermic effect at 510°C. This could represent the result of two opposite effects, which occur in the same temperature range: an exothermic one corresponding to the formation of $LaMnO_2CO_3$, an intermediate compound mentioned in literature [7] and an endothermic one corresponding to the reduction of MnO_2 into Mn_2O_3. X-ray diffraction data obtained for the powder thermally treated until 550°C confirm this statement. Another endothermic effect at ~800°C is probably due to the decomposition of the intermediate compound with formation of perovskite structure. X-ray diffraction patterns of the thermally treated powders until 850°C evidence the formation of solid solutions with perovskite structure identified by the main diffraction peaks. Actually, at this temperature the reaction is not yet accomplished, unreacted raw materials (La_2O_3 and Mn_2O_3) being identified. The thermal effect of the intermediate compound formation at 510°C is less sharp for the mixtures with dopants. The decomposition temperature of the intermediate is lower in the following order: 810°C (LM_3)>802°C (LCM_3)> 782°C (LSM_3).

In conclusion, thermal analysis associated with X-ray diffraction investigation shows different behaviors of the mixtures, as a function of the precursor used. If in case of mixtures prepared from manganese oxide and acetate precursors the formation of the perovskite structure is slow, requires a large temperature range and occurs simultaneously with the decomposition of a raw material ($La_2O_2CO_3$), in case of mixtures prepared with $MnCO_3$ as precursor, the formation of the same structure occurs at higher temperatures, as consequence of the decomposition of the intermediate $LaMnO_2CO_3$.

X-ray diffraction analysis

The phase composition and the structure of manganites for the mixtures thermally treated in isothermal conditions are listed in Table 3.

For the compositions LM_1, LM_2 and LM_3 corresponding to the undoped manganites, X-ray diffraction data evidence the formation of $LaMnO_3$ with perovskite structure at 1000°C.

$LaMnO_3$ obtained from MnO_2 as precursor exhibits the classic orthorhombic structure at this temperature. Besides this major phase, small amounts of unreacted raw materials (La_2O_3, MnO_2) were detected in all the materials obtained. This trend of a more complex phase composition at lower temperature is more important for samples resulted from MnO_2 as a consequence of its slower reactivity.

In case of mixtures with calcium (x=0.3), LCM_1, LCM_2 and LCM_3, the main diffraction lines are not splitted. This shows that this admixture favours the transition from an orthorhombic symmetry structure (Pbnm) to a structure with hexagonal one (rhombohedral, R3c). The structure distortion induced by the integration of Ca^{2+} ion could be explained in terms of ionic radii difference between the substituent and the host ions ($r_{Ca^{2+}}$=0.99 Å, $r_{La^{3+}}$=1.14 Å). This effect appears no matter of the precursor used.

Table 3 Phase composition of the samples and structure of the manganites investigated in isothermal conditions

Symbol	T/°C	Phase composition	Structure of the manganites
LM_1	1000	$LaMnO_3$ (+++), La_2O_3 (++), Mn_3O_4 (+), MnO_2 (++)	o
	1300	$LaMnO_3$ (++++)	o
LCM_1	1000	$LaMnO_3$ ss (+++), La_2O_3 (+++), Mn_3O_4 (+), MnO_2 (++)	o→h
	1300	$LaMnO_3$ ss (++++)	h
LSM_1	1000	$LaMnO_3$ ss (+++), La_2O_3 (+++), Mn_3O_4 (+), MnO_2 (+)	o→h
	1300	$LaMnO_3$ ss (++++)	h
$LCSM_1$	1000	$LaMnO_3$ ss (+++), La_2O_3 (+++), Mn_3O_4 (+), MnO_2 (+)	o→h
	1300	$LaMnO_3$ ss (++++)	h
LM_2	1000	$LaMnO_3$ (++++)	o→h
	1300	$LaMnO_3$ (++++)	h
LCM_2	1000	$LaMnO_3$ ss (++++), La_2O_3 (t), Mn_3O_4 (+)	h
	1300	$LaMnO_3$ ss(++++)	h
LSM_2	1000	$LaMnO_3$ ss (++++), La_2O_3 (t), Mn_3O_4 (+)	h
	1300	$LaMnO_3$ ss (++++)	h→c
$LCSM_2$	1000	$LaMnO_3$ ss (++++), La_2O_3 (t), Mn_3O_4 (+)	h
	1300	$LaMnO_3$ ss (++++)	h
LM_3	1000	$LaMnO_3$ (++++), La_2O_3 (+), Mn_3O_4 (+)	o→h
	1300	$LaMnO_3$ (++++)	h
LCM_3	1000	$LaMnO_3$ ss (++++), La_2O_3 (t), Mn_3O_4 (+)	h
	1300	$LaMnO_3$ ss (++++)	h
LSM_3	1000	$LaMnO_3$ ss (++++), Mn_3O_4 (+)	h
	1300	$LaMnO_3$ ss (++++)	c
$LCSM_3$	1000	$LaMnO_3$ ss (++++), Mn_3O_4 (+)	h
	1300	$LaMnO_3$ ss (++++)	h→c

(++++) – very intense; (+++) – intense; (++) – medium; (+) – weak; (t) – traces; ss – solid solution; o – orthorhombic; h – hexagonal; c – cubic

Table 4 Structural data of the manganites obtained from MnO_2 precursor and sintered at 1300°C

Symbol	a/Å	b/Å	c/Å	V/Å^3	Z	$\rho_{theoretical}$	Structure
LM_1	5.4383	5.5116	7.7264	231.589	4	6.934	orthorhombic
LCM_1	5.4491	–	13.3306	342.791	6	6.095	hexagonal
LSM_1	5.5036	–	13.3067	349.056	6	6.393	hexagonal
$LCSM_1$	5.4892	–	13.3738	348.982	6	6.190	hexagonal

For the LSM samples (with strontium admixture) one can notice a weaker effect concerning the splitting of the peaks at low temperature (1000°C) caused by a less important structure distortion induced by strontium. This fact can be explained by taking into account the ionic radius of strontium ($r_{Sr^{2+}}$=1.12 Å), higher than that of calcium one. Thus, while $CaMnO_3$ is totally soluble in $LaMnO_3$ [8], $SrMnO_3$ has a

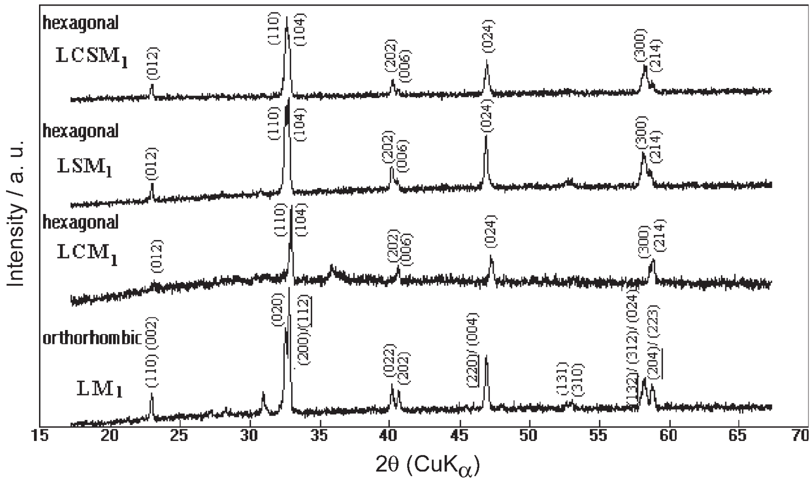

Fig. 4 X-ray diffraction patterns of manganites obtained by using of MnO_2 precursor and thermally treated at 1300°C

solubility limit in $LaMnO_3$ corresponding to x=0.4 [9]. At higher temperatures the strontium incorporation increases significantly and determines therefore a strong distortion, the structure of the resulted samples being a cubic one.

At 1300°C all the materials are single phase with a perovskite structure more or less distorted as a function of the presence and type of admixture (Fig. 4).

The X-ray diffraction analysis shows a distortion of the orthorhombic structure corresponding to the pure compound towards a structure with hexagonal (rhombohedral) symmetry corresponding to the mixed crystals obtained by integration of the alkaline earth ions. This phase transition is accompanied by a significant increase of the unit cell volume due to its extension along the *c* axis.

IR spectroscopy

The data corresponding to the samples thermally treated at 1300°C confirm the X-ray diffraction results (Fig. 5). The introduction of alkaline earth admixtures leads to the flattening and shift of the 612 cm^{-1} characteristic band as a consequence of the streching motion of oxigen atoms in the *ab* plane of the MnO_6 octahedra. The increase of the symmetry degree determines the decrease of the phononic modes of IR spectra. More important structure changes are evidenced by using of manganese acetate and carbonate as precursors. In case of strontium admixture the vibration band characteristic of the hexagonal structure is missing, thus, showing a clear change towards the cubic structure. This effect was mentioned in literature for lanthanum manganites with barium admixture [10].

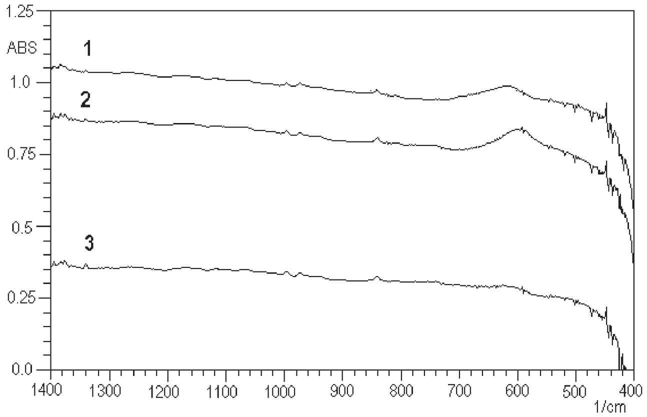

Fig. 5 IR spectra of manganites obtained from $Mn(CH_3COO)_2$ precursor: 1 – LM_2; 2 – LCM_2; 3 – LSM_2

Conclusions

- Thermal analysis data pointed out different behaviors of the mixtures as a function of the type of manganese precursor used. Thus, in case of the mixtures obtained by using of MnO_2 and $Mn(CH_3COO)_2$ as precursors, the formation of the perovskite structure is slower and occurs in a large temperature range simultaneously with the decomposition of a raw material ($La_2O_2CO_3$). Unlike, in case of the mixtures prepared from $MnCO_3$, the formation of the perovskite type structure takes place at a higher temperature as a consequence of an intermediate compound ($LaMnO_2CO_3$) decomposition;
- X-ray diffraction data revealed a pronounced trend to non-stoichiometry of the compositions mentioned. Thus, as a function of the solute type, a mixture of manganites with different perovskite structures was formed. While calcium is solubilized at lower temperatures (1000°C) determining an orthorhombic→hexagonal transition, the effect of strontium is important at higher temperatures (1300°C) when a perovskite phase with cubic structure becomes prevalent (for $MnCO_3$ and $Mn(CH_3COO)_2$ precursors);
- The IR spectroscopy data are in fair good agreement with the diffraction results; the phase transitions mentioned are clearly emphasized by a gradual flattening of the characteristic band corresponding to the MnO_6 octahedra until its disappearance with the increase of the symmetry degree of the solid solutions formed (especially for Sr-doped manganites).

References

1 N. Q. Minh, J. Am. Ceram. Soc., 76 (1993) 563.
2 T. Yao, T. Ito and T. Kokubo, J. Mater. Res., 10 (1995) 1079.
3 J. A. M. van Roosmalen, P. van Vlaanderen and E. H. P. Cordfunke, J. Solid State Chem., 114 (1995) 516.

4 R. Mahendiran, S. K. Tiwary, A.K. Raychaudhuri, T. V. Ramakrishnan, R. Mahesh, N. Rangavittal and C.N.R. Rao, Phys. Rev. B, 53 (1996) 3348.
5 M. Hervieu, R. Mahesh, N. Rangavittal and C. N. R. Rao, Eur. J. Solid State Inorg. Chem., 32 (1995) 79.
6 S. Bilger, E. Syskakis, A. Naoumidis and H. Nickel, J. Am., Ceram. Soc., 75 (1992) 964.
7 I. Maurin, P. Barboux, Y. Lassailly, J. P. Boilot and F. Villain, J. Magnetism and Magn. Mat., 211 (2000) 139.
8 P. Schiffer, A. P. Ramirez, W. Bao and S.-W. Cheong, Phys. Rev. Lett., 75 (1995) 3336.
9 A. Urushibara, Y. Moritomo, T. Arima, A. Asamitsu, G. Kido and Y. Tokura, Phys. Rev. B, 51 (1995) 14103.
10 C. Roy and R.C. Budhani, J. Appl. Phys., 85 (1999) 3124.